

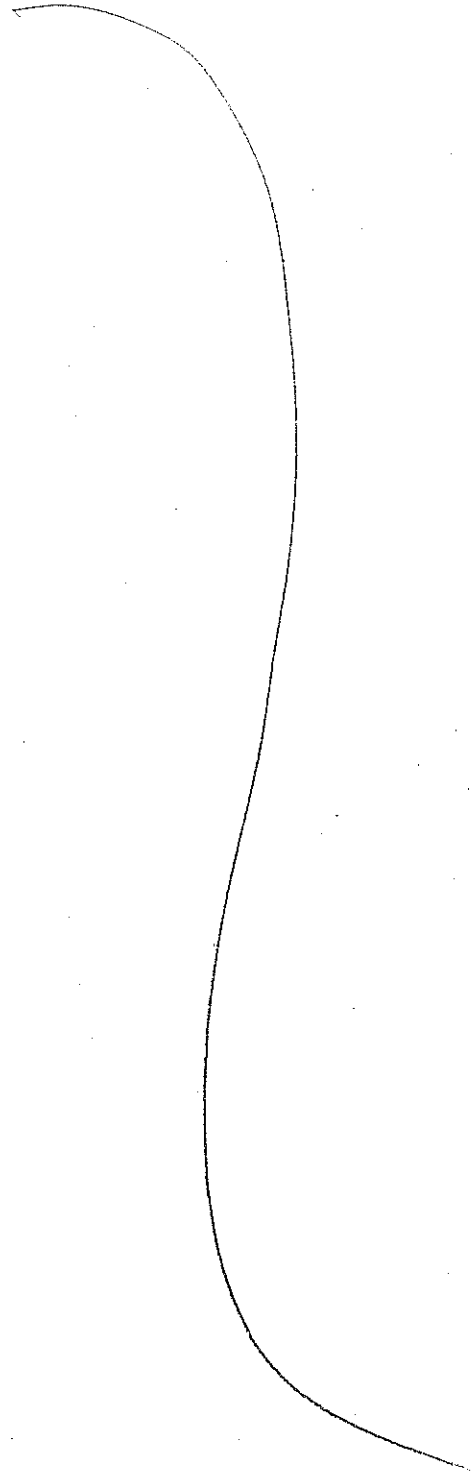
In the calculation of absolute nuclear reaction cross section two elements melt together: reaction and structure.

In the case of weakly coupled probes like, as a rule, one-particle transfer processes are, the first element can be divided into two essentially separated components: elastic scattering (optical potentials), and transfer amplitudes connecting entrance and exit channels. In other words, the habitat of DWBA.

In Fig. 6.2.1(a) a concrete embodiment of the formalism presented in the first part of this Chapter worked out with the help of the software ONE (Potel 2012), of global optical parameters (Dickey et al 1982) and of NFT spectroscopic amplitudes (cf. Table 6.2.1), is given. In it, the absolute differential cross section associated with the population of the low-lying state $|^{119}\text{Sn}(1/2^-; 88\text{keV})\rangle$ in the one-particle pick-up process $^{120}\text{Sn}(p,d)^{119}\text{Sn}$ is compared with the experimental data.

Potel 2012, Potel, G. ONE: one-particle transfer software (DWBA) for both light and heavy ions, private communication.

In Fig. 6.2.1(b) the theoretical predictions obtained with the help of ONE are compared to those calculated making use of the same spectroscopic amplitude and optical potential the software FRESCO (Thompson 1988). (2)



Similar calculations (ONE, NFF spectroscopic amplitudes and global optical parameters), have been carried for the reaction $^{120}\text{Sn}(d,p)^{121}\text{Sn}(j^\pi; E_x)$ in connection with the population of the $1\frac{3}{2}^+; g.s.$ and $1\frac{1}{2}^-; E_x \approx 0 \text{ MeV}$ states. (Bechara et al 1977)

In the stripping experiment the ground state and the $1\frac{1}{2}^-$ state were not resolved in energy. This is the reason why theory and experiment are only compared to the data for the summed $l=0+5$ differential cross section (cf. Fig. 6.2.2 (a)), the separate theoretical predictions been displayed in Figs. 6.2.2 (b) and (c).

Let us now turn to the most fragmented low-lying quasiparticle state around ^{120}Sn , namely that associated with the $d_{5/2}$ orbital (cf Idini 2012, Idini et al 2012).

Bechara MJ and O. Dietzsch, States in ^{121}Sn from the $^{120}\text{Sn}(d,p)^{121}\text{Sn}$ reaction at 17 MeV, Phys. Rev. 12, 90, 1975

Idini A, Renormalization effects in Nuclei, <http://air.unimi.it/handle/2434/216315>

Idini, A, F. Barranco and E. Vigezzi, Phys. Rev. C85, 014331, 2012

In fact, five low-lying $5/2^+$ states have ⁽⁴⁾
been populated in the reaction $^{120}\text{Sn}(p,d)^{119}\text{Sn}$
with a summed cross section $\sum_{i=1}^5 \sigma(2^\circ-25^\circ)$
 $\approx 8 \text{ mb} \pm 2 \text{ mb}$ (Dickey et al 1982), while
four are theoretically predicted with
 $\sum_{i=1}^4 \sigma(2^\circ-25^\circ) = 6.2 \text{ mb}$ (see Fig. 6.2.3)
(cf. also Idini et al 2014).

This is likely to be, within the present
context, namely that of probing the
single-particle content of an elemen-
tary excitation, a rather trying situation,
and provides a measure of the limita-
tions encountered by such a quest.

Analysis of the type presented above
allows one to posit that structure and
reactions are but just two aspects of
the same physics. If one adds to this
picture the fact that the optical potential - that is,
the energy and momentum dependent
nuclear dielectric function describing
the medium where direct nuclear
chemistry takes place - can be
calculated microscopically, in terms

(artículo ruso
90 años Belyaev)

(cf. refs. [44]-[51])

Idini, A., G. Potel, F. Barranco, E. Vigezzi
and R. A. Broglie, Dual Origin of
pang in nuclei, ArXiv - -

(5)

of the same elements entering structure calculations (i.e. spectroscopic amplitudes, single-particle wavefunctions, transition densities and eventually effective formfactors), the structure reaction loop closes itself.

If one allows for halos to be part of the daily nuclear structure paradigm, the equivalence between structure and reaction becomes even stronger, explaining in simple terms why one-particle transfer is likely to be, as a rule, the main channel contributing to the entrance channel deuteronation (absorptive optical potential), in keeping with the large overlap displayed the corresponding single-particle wavefunctions, as compare to particle-hole configuration controlling inelastic processes (cf. Fig. 2.B.3).

Searching for further contact points between structure and reactions, one can posit that the above parlance, although being essentially correct, does not emphasize enough the central role virtual, correlated particle-hole excitations play in the single-particle transfer process. In fact, as a result of the interweaving of single-particle (quasi-particle) motion and e.g. collective surface vibrations, particles become dressed, being able to contribute less (differently) to the direct transfer process but, eventually, opening new doorway channels (states) (cf. Feshbach 1958, Rawistcher 1989, Bertsch et al 1983, Bortignon et al 1981) to deprotonate the entrance channel (cf. e.g. figurita 1 D 4 de la introduction, Jaulitas), similar to those responsible for the breaking of the single-particle strength ($Z_w (= m/m_w)$) and damping giant resonances and renormalizing low-lying collective

states (cf. G.C. 2 and G.C. 3, G.E. 1 and G.E. 2).

(7)

It seems then fair to say that the importance of the coupled channel approach to reactions (cf. e.g. Thompson 1988, 2013 (refs. [73] and [77] Review paper), Tamura 1970, Ascutto and Glendenning 1969, 1970, 1970 b, 1971, 1972; cf. also [46], [47] art. VUSO Belyaev 90 years) A. Moro et al

is not so much, or at least not only, that it is able to handle situations like for example one-particle transfer to members of a rotational band, alas at the expense of eventually adjusting the optical potential, but that it reminds us how intimately connected in nuclei, probe and probed are.

On the other hand for most of the situations dealt in the present monography, it is transparent the power of perturbative DWBA (e.g. 1st for one-nucleon transfer), also to reflect the physics,

and 2nd for Cooper pair tunneling),^⑧
coupled together with NFT elementary
modes of nuclear excitation
approach.

To which extent a FRESCO-
like software built on a NFT
basis will ever be attempted
is an open question. Note in any
case the serious attempts made
at incorporating so called core
excitations within the FRESCO
framework ([46, 47] Belyaev 90
article, AMoro et al)

(6)

		$^{120}\text{Sn}(p,d)^{119}\text{Sn}(g)$	$^{120}\text{Sn}(d,p)^{121}\text{Sn}(g)$
J	$E_J(\text{MeV})$	\overline{U}_J^2	\overline{U}_J^2
$h_{11/2}$	1.54	(1.34) 0.25 (0.28)	(1.25) 0.55 (0.49)
$d_{3/2}$	1.27	(1.27) 0.35 (0.41)	(1.25) 0.41 (0.44)

Table 62.1

The properties of the main peaks of the $h_{11/2}$ and $d_{3/2}$ strength functions of ^{120}Sn calculated taking into account the interweaving of fermionic and bosonic elementary modes of excitation within NFT and their consequences in both the normal and abnormal densities (cf Idini 2012; Idini et al 201; see also Idini et al 2014 where the spin degrees of freedom, solely repulsive pairing channel (1S_0) in finite nuclei, has also been included).

In parenthesis, experimental (energies) and empirical (single-particle strength) data are given (Bechara et al, 1975; Dufay et al, 1982).

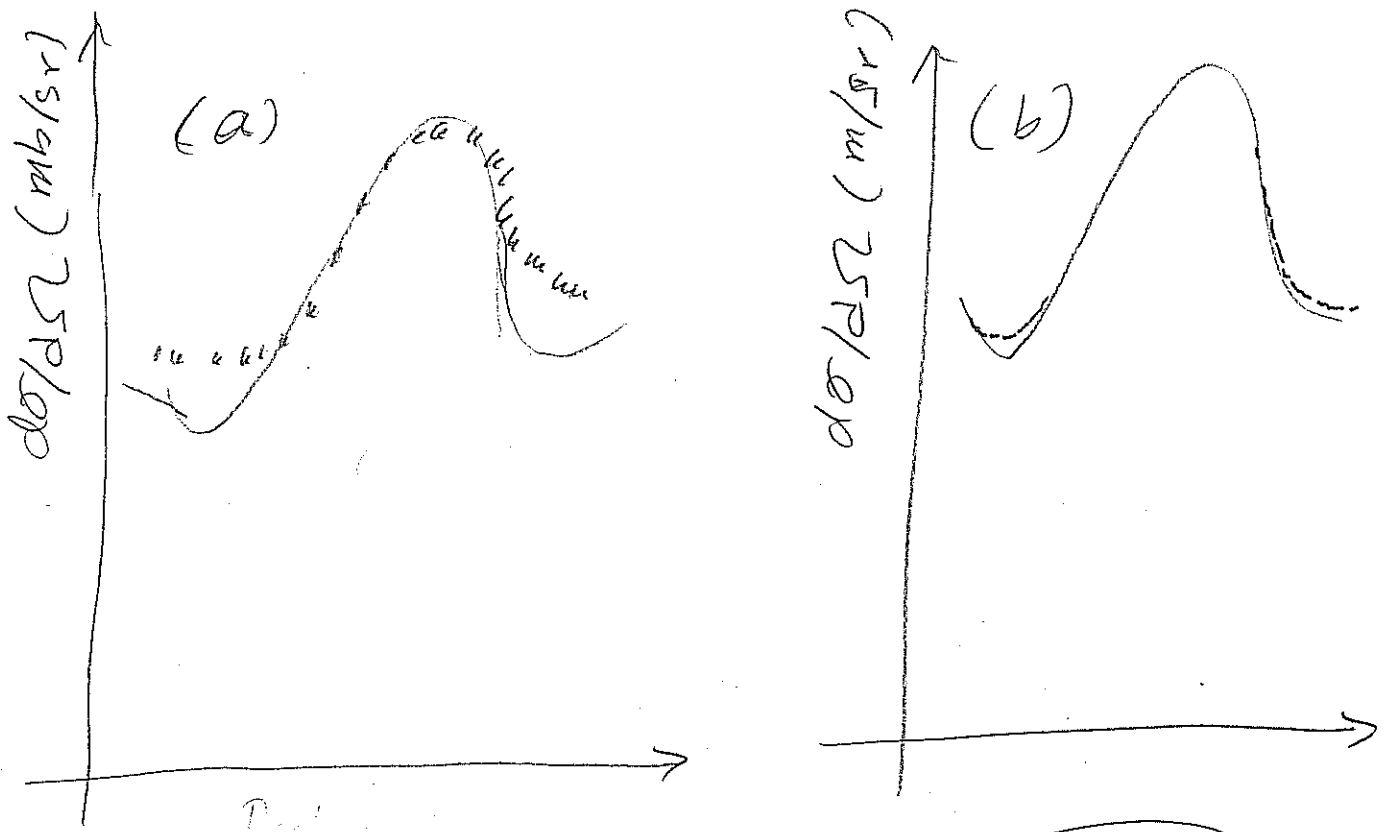


Fig. 6.2.1

The absolute differential cross section $^{120}\text{Sn}(p,d)^{119}\text{Sn}(j^\pi)$ associated with the state $j^\pi = 11/2^-$. (a) the theoretical predictions discussed in the text ^{are displayed in} comparison with the experimental data. The corresponding integrated cross sections are 5.0 and 5.2 ± 0.6 mb respectively. (b) The same theoretical differential cross section ~~is compared with~~ mentioned above is given together with the results of the software FRESKO making use again of the ^(NFT) spectroscopic amplitudes.

(Dichev et al 1982)

(8)

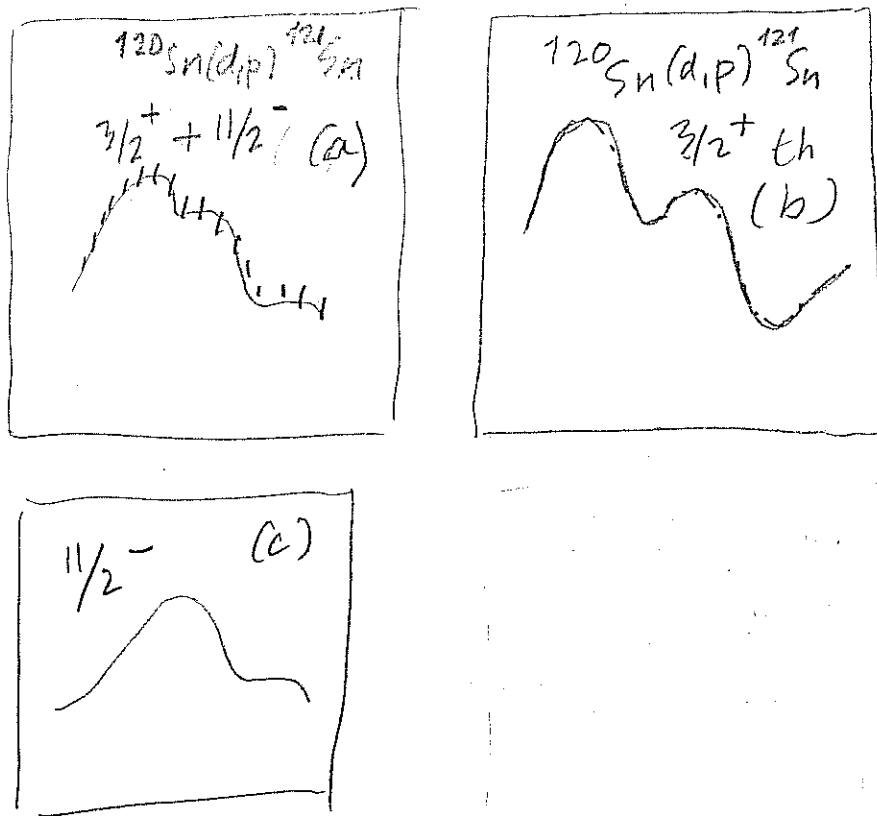


Fig. 6.2.2

absolute differential cross section
 The theoretical angular distributions associated with the reaction $^{120}\text{Sn}(d,p)^{121}\text{Sn}$ and populating the low-lying states $3/2^+$ and $11/2^-$ are shown in (b) and (c), while the summed differential cross sections are ~~also~~ is displayed in (a) in comparison with the data (Bechara et al, 1975)

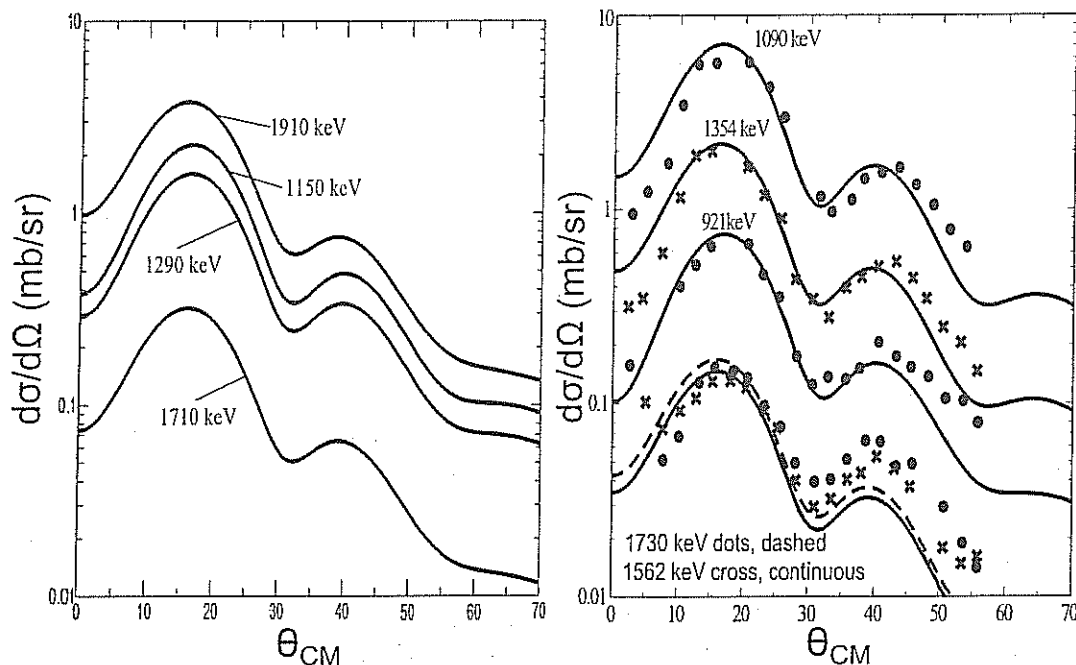


FIG. 6. $^{120}\text{Sn}(p, d)^{119}\text{Sn}(5/2^+)$ absolute experimental cross sections [19] (dots), together with the DWBA fit carried out in the analysis of the data (right panel), in comparison with the finite range, full recoil DWBA calculations carried out with the help of state of the art optical potential and v_{np} interaction (I. Thompson, private communication), making use of the NFT structure inputs as explained in the text.

J.

I.J. Thompson

~~1562~~
~~1090~~
~~472~~

~~1910~~
~~1354~~
~~921~~